



1 Lability classification of soil organic matter in the northern permafrost region

2
3 *Kuhry, Peter¹, Bárta, Jiří², Blok, Daan³, Elberling, Bo⁴, Faucherre, Samuel⁴, Hugelius,*
4 *Gustaf^{1,5}, Richter, Andreas⁶, Šantrůčková, Hana² and Weiss, Niels^{1,7}*

5
6 ¹⁾ Department of Physical Geography, Stockholm University, Sweden

7 ²⁾ Department of Ecosystem Biology, University of South Bohemia, Ceske Budejovice, Czech Republic

8 ³⁾ Department of Physical Geography and Ecosystem Science, Lund University, Sweden

9 ⁴⁾ CENPERM, University of Copenhagen, Denmark

10 ⁵⁾ Bolin Centre for Climate Research, Stockholm University, Sweden

11 ⁶⁾ Department of Microbiology and Ecosystem Science, University of Vienna, Austria

12 ⁷⁾ Current affiliation: Department of Geography and Environmental Studies, Carleton University, Ottawa, Canada

13
14 Correspondence email: peter.kuhry@natgeo.su.se

15 16 Abstract

17
18 The large stocks of soil organic carbon (SOC) in soils and deposits of the northern permafrost region
19 are sensitive to global warming and permafrost thawing. The potential release of this carbon (C) as
20 greenhouse gases to the atmosphere does not only depend on the total quantity of soil organic matter
21 (SOM) affected by warming and thawing, but also on its lability (i.e. the rate at which it will decay).
22 In this study we develop a simple and robust classification scheme of SOM lability for the main
23 types of soils and deposits of the northern permafrost region. The classification is based on widely
24 available soil geochemical parameters and landscape unit classes, which makes it useful for
25 upscaling to the entire northern permafrost region. We have analyzed the relationship between C
26 content and C-CO₂ production rates of soil samples in two different types of laboratory incubation
27 experiment. In one experiment, c. 240 soil samples from four study areas were incubated using the
28 same protocol (at 5 °C, aerobically) over a period of one year. Here we present C release rates
29 measured on day 343 of incubation. These long-term results are compared to those obtained from
30 short-term incubations of c. 1000 samples (at 12 °C, aerobically) from an additional three study
31 areas. In these experiments, C-CO₂ production rates were measured over the first four days of
32 incubation. We have focused our analyses on the relationship between C-CO₂ production per gram
33 dry weight per day (µgC-CO₂ gdw⁻¹ d⁻¹) and C content (%C of dry weight) in the samples, but show
34 that relationships are consistent when using C/N ratios or different production units such as µgC per
35 gram soil C per day (µgC-CO₂ gC⁻¹ d⁻¹) or per cm³ of soil per day (µgC-CO₂ cm³⁻¹ d⁻¹). C content of
36 the samples is positively correlated to C-CO₂ production rates but explains less than 50 % of the
37 observed variability when the full datasets are considered. A partitioning of the data into landscape
38 units greatly reduces variance and provides consistent results between incubation experiments. These
39 results indicate that relative SOM lability decreases in the order: Late Holocene eolian deposits >
40 alluvial deposits and mineral upland soils (including peaty wetlands) > Pleistocene Yedoma deposits
41 > C-enriched pockets in cryoturbated soils > peat deposits. Thus, three of the most important SOC
42 storage classes in the northern permafrost region (Yedoma, cryoturbated soils and peatlands) show
43 low relative SOM lability. Previous research has suggested that SOM in these pools is relatively
44 undecomposed and the reasons for the observed resistance to decomposition in our experiments
45 needs urgent attention if we want to better constrain the magnitude of the thawing permafrost carbon
46 feedback on global warming.

47

48 1. Introduction

49

50 Permafrost has been recognized as one of the vulnerable carbon (C) pools in the Earth System
51 (Gruber et al., 2004). In the most recent decade there has been a surge in papers dealing with the
52 permafrost carbon feedback on climate change (e.g. Schuur et al., 2008; Kuhry et al., 2010). This
53 increased interest was fueled by a new and high estimate of the total soil organic carbon (SOC)
54 storage in the northern permafrost region (Tarnocai et al., 2009), which was received with great
55 interest by the Earth System Science community (e.g., Ciais, 2009). Since this first new estimate was
56 published, a multitude of new SOC inventories at the landscape level have been conducted across the
57 Circumpolar North (e.g. Hugelius and Kuhry, 2009; Hugelius et al., 2010; Horwath Burnham and
58 Sletten, 2010; Palmtag et al., 2015; Gentsch et al., 2015; Siewert et al., 2016). Recent studies have
59 also focused on re-evaluating the spatial extent and SOC storage of the Yedoma ‘Ice Complex’ and
60 Alas deposits (Strauss et al., 2013; Walter-Anthony et al., 2014; Hugelius et al., 2016; Shmelev et al.,
61 2017).

62 This new data has prompted an update of the total SOC storage in the northern permafrost
63 region, its vertical partitioning and its broad (continental scale) distribution (Hugelius et al., 2014).
64 The new estimate amounts to c. 1400 PgC for the top 3 m of soils and deeper deposits, including
65 permafrost and non-permafrost organic soils (Histels/Histosols, 302 PgC), cryoturbated permafrost
66 mineral soils (Turbels, 476 PgC), non-cryoturbated permafrost mineral soils (Orthels) and non-
67 permafrost mineral soils (256 PgC), and deeper Yedoma (301 PgC, >300 cm) and Delta (91 PgC,
68 >300 cm) deposits. The spatial distribution of SOC stocks according to the major permafrost soil
69 (Gelisol) suborders, non-permafrost mineral soils and Histosols (Soil Survey Staff, 2010) is
70 graphically represented in the updated version of the Northern Circumpolar Soil Carbon Database
71 (NCSCDv2, 2014).

72 The importance of an accurate estimate of total SOC storage in the northern permafrost region is
73 illustrated by a recent review of the permafrost carbon feedback (Schuur et al., 2015), which
74 included a comparison of future C release in a total of eight Earth System models (ESMs). The
75 magnitude of the projected cumulative C loss from thawing permafrost by 2100, largely based on the
76 RCP 8.5 scenario (IPCC, 2013), varied greatly between models from 37 to 174 PgC. However, by
77 normalizing for the initial permafrost C pool size in the different ESMs, the proportional C loss from
78 the permafrost zone was constrained to a much narrower range of 15 ± 3 % of the initial pool. This
79 indicates that the quantity of SOC is a primary control when assessing C losses from the northern
80 permafrost region.

81 The magnitude of the permafrost carbon feedback, however, will not only depend on the rate of
82 future global warming (and its polar amplification), its effect on gradual and abrupt permafrost
83 thawing (Grosse et al., 2011), or the total size (and vertical distribution) of the permafrost SOC pool.
84 As shown by Burke et al. (2012), based on simulations with the Hadley Centre climate model,
85 quality (decomposability) parameters need also to be considered. Thus, in terms of C pool
86 parameters, the potential C release from the northern permafrost region will depend not only on SOC
87 quantity but also on soil organic matter lability (i.e. the rate at which SOM will decay following
88 warming and thawing). An important tool to assess potential C release from permafrost soils and
89 deposits are laboratory incubation experiments that consider both different types of substrate (e.g.,
90 Schädel et al., 2013) and time of incubation (e.g. Elberling et al., 2013).

91 The aim of this study is to add a measure of SOM lability to the current estimates of SOC
92 quantity, in order to define vulnerable C pools across the northern circumpolar region. We focus on
93 the relationship between solid phase geochemical parameters (particularly C content) and C release
94 rates in laboratory incubations of active layer and thawed permafrost samples from the main types of
95 soils and deposits found in the northern permafrost region. Our objective is to develop a SOM
96 lability classification scheme based on widely reported soil geochemical parameters in field SOC



97 inventories and general landscape classes, that can be linked to existing spatial SOC databases such
98 as the NCSCD (Tarnocai et al., 2009; Harden et al., 2012; Hugelius et al., 2014). We test the
99 robustness of our SOM lability classification by comparing two very different types of incubation
100 experiment, both in setup as well as timing of C release measurements.

101

102 2. Materials and methods

103

104 *2.1. Study areas*

105

106 The samples used in the incubation experiments were collected as part of landscape-level inventories
107 carried out in the context of the EU PAGE21 and ESF CryoCarb projects to assess total storage,
108 landscape partitioning and vertical distribution of SOC stocks in study areas across the northern
109 permafrost region. SOC storage data from these areas are published in Weiss et al. (2017) for
110 Svalbard, Siewert et al. (2016) for Lena Delta, Palmtag et al. (2016) for Taymyr Peninsula, Palmtag
111 et al. (2015) for Lower Kolyma, Hugelius et al. (2011) for Seida, and Siewert (2018) for Stordalen
112 Mire. The location of all study areas is shown in Fig. 1. The Lower Kolyma experiment includes
113 samples from two nearby located study areas (Shalaurovo and Cherskij); the Taymyr Peninsula
114 experiment also includes samples from two nearby located study areas (Ary-Mas and Logata).
115 Metadata for each of these areas, including geographic coordinates, permafrost and vegetation zones,
116 climate parameters, number of soil profiles and incubated samples, type of incubation experiment,
117 and time of field collection, are presented in Table S1 (Supplementary Materials).

118

119 Figure 1. Location of study areas in northern Eurasia. PAGE21 experiment (Ny Ålesund,
120 Adventdalen, Stordalen Mire, Lena Delta); CryoCarb 1-Kolyma experiment (Shalaurovo,
121 Cherskij); CryoCarb 2-Taymyr experiment (Ary-Mas, Logata); CryoCarb 3-Seida experiment.
122 Permafrost zones according to Brown et al. (1997).

123

124 *2.2. Field methods*

125

126 The sampling strategy applied for SOC field inventories was aimed at capturing all major landscape
127 units in each of the study areas, while at the same time ensuring an unbiased selection of soil profile
128 location. This semi-random sampling approach consisted of deciding on the positioning of generally
129 1 or 2 km long transects that crossed all major landscape units, with a strictly equidistant sampling
130 interval at normally 100 or 200 m that eliminated any subjective criteria for the exact location of
131 each soil profile. For SOC storage calculations, the mean storage in each landscape unit class was
132 weighed by its proportional representation in the study area based on remote sensing land cover
133 classifications.

134 At each soil profile site, the topsoil organic layer was collected by cutting out blocks of known
135 volume in three random replicates to account for spatial variability. These samples do not always
136 strictly adhere to the definition of an 'O' soil genetic horizon, because in areas with thin topsoil
137 organics (like in floodplains and mountain terrain) there can be a large admixture of minerogenic
138 material resulting in C contents of less than 12 %. Active layer samples were collected from
139 excavated pits by horizontally inserting fixed-volume cylinders. The permafrost layer was sampled
140 by hammering a steel pipe of known diameter incrementally into the ground, retrieving intact
141 samples for each depth interval. Depths intervals are normally 5 to 10 cm or less (e.g., when the
142 topsoil organic layer was very thin). The standard sampling depth was 1 m below the soil surface; at



143 some sites it was not possible to reach this depth due to large stones in the soil matrix or thin soil
144 overlying bedrock (often in mountainous settings).

145

146 2.3. Incubation experiments

147

148 2.3.1. The PAGE21 incubation experiment

149

150 The PAGE21 incubation experiment was carried out at the University of Copenhagen (Denmark).
151 This experiment included one sample from the topsoil organics, one sample from the middle of the
152 active layer and one sample from the upper permafrost layer (normally 10-15 cm below the upper
153 permafrost table) from all mineral soil profiles collected in three of the PAGE21 study areas.
154 Samples were selected based on depth criteria and not any specific soil characteristic (e.g., presence
155 of C-enriched cryoturbated material or absence of excess ground ice). In some cases, upper
156 permafrost samples could not be collected due to very deep active layers and/or thin soils
157 (particularly in mountain settings). Peat samples are available from a fourth PAGE21 study area. In
158 total c. 240 soil samples from four study areas across the northern permafrost region (Ny Ålesund
159 and Adventdalen, Svalbard; Stordalen Mire, N Sweden; Lena Delta, N Siberia) were incubated in
160 one and the same experiment (Faucherre et al., 2018).

161 The Dry Bulk Density (DBD) of samples used for incubation was measured at Stockholm
162 University (Sweden). The %C and %N of dry weight of the incubated samples were measured in an
163 elemental analyzer (EA Flash 2000, Thermo Scientific, Bremen, Germany) at the University of
164 Copenhagen (Denmark).

165 Samples were kept in frozen condition from collection until the start of the laboratory incubation
166 experiment. Samples were incubated at 5 °C and field water content levels (aerobic conditions) over
167 a one-year time period. Mean volumetric water content varied between 30 % (topsoil organics), 45-
168 50 % (active layer and permafrost layer mineral soil) and 69 % (peat). C-CO₂ production rates were
169 measured at five different occasions between 7 to 343 days after the start of the experiment, using a
170 nondispersive infrared LI-840A CO₂/H₂O Gas analyzer (LICOR® Biosciences). Here, we use C
171 release rates after nearly one year of incubation as a measure of SOM lability. Since all samples from
172 all study areas were processed and incubated using the same protocol, results are directly
173 comparable.

174

175 2.3.2. The CryoCarb incubation experiments

176

177 The CryoCarb incubations were carried out at the University of South Bohemia (Ceske Budovice,
178 Czech Republic). These experiments included all samples from all profiles collected in each of three
179 study areas (CryoCarb 1-Kolyma in NE Siberia; CryoCarb 2-Taymyr in N Siberia; and CryoCarb 3-
180 Seida in NE European Russia). In total c. 1000 samples were incubated.

181 The Dry Bulk Density (DBD) of samples used for incubation was measured at Stockholm
182 University (Sweden). The %C and %N of dry weight were measured in an EA 1110 Elemental
183 Analyzer (CE Instruments, Milan, Italy) at Stockholm University (Seida samples) and the University
184 of Vienna (Kolyma and Taymyr samples).

185 Collected soil samples were dried at 40-50 °C within two weeks after field sampling and kept in
186 a cold room until analyzed. Dry soil (0.2 g) was mixed with 1.6 ml of soil inoculum (soil:H₂O,
187 1:100, weight/volume) in 10 ml vacutainers, after which the vacutainers were hermetically closed
188 and the soil slurry was incubated in an orbital shaker at 12 °C for 96 hours. At the end of incubation,
189 CO₂ concentration in the headspace was analyzed using an HP 5890 gas chromatograph (Hewlett-



190 Packard, USA), equipped with a TC detector. The soil inoculi were prepared from samples of fresh
191 soil taken separately from topsoil organic layer, mineral/peat active layer and mineral/peat
192 permafrost layer, from soil profiles collected in each study area. The fresh soil was kept in a cold
193 room and then conditioned at 15 °C for one week before inoculum preparation. Samples were
194 incubated with inoculum prepared from the respective soil horizons.

195 In the CryoCarb experiments, short term C-CO₂ production rates after rewetting of dried soil
196 samples was used as an indicator of SOM lability. It is well documented that C is released after
197 rewetting of dry soil, the amount of which is site and soil type specific and represents the available
198 fraction of soil C (Fierer and Schimel, 2003; Franzluebbers et al., 2000; Šantrůčková et al., 2006).
199 Due to different sample pretreatment, including duration until drying and incubation experiment, as
200 well as the different ‘local’ soil inoculi used, we consider the CryoCarb incubations of the three
201 different study areas as separate experiments.

202

203 *2.4. Geochemical parameters and C-CO₂ production rates*

204

205 As potential explanatory geochemical parameters we have considered dry bulk density (DBD),
206 carbon content (%C of dry weight) and carbon to nitrogen weight ratios (C/N). In this study, we
207 focus on the relationship between %C in samples and the corresponding C-CO₂ production in aerobic
208 incubation experiments. An important practical reason is that %C is most widely available since it
209 can be derived with a high degree of confidence from Elemental Analysis, but also from indirect
210 methods such as loss-on-ignition at 550 °C. However, there are also theoretical considerations for the
211 choice of %C. DBD is expected to be related to quantity and degree of compaction (decomposition)
212 of SOM. However, in the permafrost layer of soils it will also co-vary with the volume of excess
213 ground ice. C/N is a good indicator of degree of SOM decomposition in peat deposits (Kuhry and
214 Vitt, 1996) and tundra upland soils (Ping et al., 2008). Recent soil carbon inventories in permafrost
215 terrain have shown a clear decrease in soil C/N as a function of age/depth (e.g., Hugelius et al., 2010;
216 Palmtag et al., 2015). However, C/N is also sensitive to original botanical composition of the
217 peat/soil litter. In contrast, the %C of plant material is much more narrowly constrained to around 50
218 % of dry plant matter. For instance, based on data in Vardy et al. (2000), we can calculate a C/N
219 range of 48.5 ± 27.9 (mean and standard deviation) in modern phytomass samples from permafrost
220 peatlands in the Canadian Arctic (n=27) that included vascular plants, mosses and lichens. The
221 corresponding %C range was much narrower at 47.3 ± 5.1 . An additional benefit of using %C is that
222 it has a clear ‘zero’ intercept in regressions against C-CO₂ production per gram dry weight per day
223 (i.e., at zero %C in soil samples we can expect zero C release). This is also the reason why
224 expressing C release as a function of gram dry weight (gdw) is more straightforward than against
225 gram C (gC). The latter would have the benefit of expressing C release directly as a function of C
226 stock, but the relationship is complex with recent studies showing high initial C release rates per gC
227 at low %C values (Weiss et al., 2016; Faucherre et al., 2018). In this study DBD is available for all
228 samples, and we can also express C release as a function of soil volume (cm³). In the results we
229 primarily show $\mu\text{gC-CO}_2$ production per gdw per day ($\mu\text{gC-CO}_2 \text{ gdw}^{-1} \text{ d}^{-1}$) as a function of %C in
230 the sample. However, in the Supplementary Materials we also refer to regressions against C/N and
231 C-CO₂ production rates per gC per day ($\mu\text{gC-CO}_2 \text{ gC}^{-1} \text{ d}^{-1}$) or per cm³ of soil per day ($\mu\text{gC-CO}_2 \text{ cm}^{-3}$
232 d^{-1}) against %C to test the robustness of our results.

233

234 *2.5. Landscape partitioning*

235

236 We have investigated C-CO₂ production rates for the full datasets as well as for samples grouped into
237 landscape unit classes that can be used for an assessment of vulnerable C pools at northern



238 circumpolar levels. For this purpose, we have subdivided our datasets to reflect the main Gelisol
239 suborders, non-permafrost mineral soils and Histosols recognized in the spatial layers of the
240 NCSCD, as well as deeper Quaternary deposits for which there are separate estimates of spatial
241 extent, depth and SOC stocks (Tarnocai et al., 2009; Strauss et al., 2013; Hugelius et al., 2014). We
242 identify the following landscape classes: peat deposits (Histels, and some Histosols), peaty wetland
243 deposits (mostly Histic Gelisols), mineral soils (Turbels and Orthels, and some non-permafrost
244 mineral soils), fluvial/deltaic (alluvial) deposits, and eolian/Yedoma deposits. Special attention is
245 paid to the lability of SOM in Holocene peat deposits, in deeper C-enriched buried layers and
246 cryoturbated pockets, and in Pleistocene Yedoma deposits. All classes are represented in the
247 PAGE21 and CryoCarb 1-Kolyma incubation experiments. The CryoCarb 2-Taymyr dataset lacks
248 sites with eolian parent materials, whereas the CryoCarb 3-Seida dataset does not include soils
249 formed into either alluvial or eolian deposits. We, therefore, focus on results from the PAGE21 and
250 CryoCarb 1-Kolyma experiments but present the main results from the two other experiments in the
251 Supplementary Materials.

252

253

2.6. Statistics

254

255 Relationships between C-CO₂ production rates and geochemical parameters for all samples, as well
256 as for groupings of samples into landscape unit classes, for each incubation experiment separately,
257 are statistically analyzed using linear, polynomial and other non-linear regressions in the Microsoft
258 Excel 2010 and Past3 (Hammer et al., 2001) software packages. Regressions are considered
259 significant if $p < 0.05$. These analyses visualize SOM lability for full profiles including samples from
260 topsoil organic to mineral layers that have a wide range of DBD, %C and C/N values. In some cases,
261 replicates are not normally distributed (or even unimodal) and statistics should be interpreted with
262 caution. This is particularly the case in peatland profiles, with clusters of samples with low DBD and
263 high %C and C/N in the peat and opposite trends in samples of the underlying mineral subsoil.

264 To alleviate the issue on non-normal distributions, C-CO₂ production rates in samples as a
265 function of %C are also tested grouped into soil horizons. This approach yields classes that are much
266 better constrained in terms of %C values. Because data were still not fully normally distributed, non-
267 parametrical Mann-Whitney tests were used (Hammer et al., 2001). The data were log-transformed
268 to reduce skewness in data distributions and to reduce the influence of fractional data. For this
269 approach, we express C-CO₂ production rates per gC to take into account the large differences in %C
270 among the different soil horizon classes. The tests are run to evaluate null hypotheses regarding
271 differences in SOM lability between soil horizon classes, with a focus on those that are considered
272 typical for specific landscape classes (C-enriched pockets for Turbels, peat samples for Histels and
273 loess samples for Pleistocene Yedoma).

274

275

3. Results

276

277

3.1. Simple geochemical indicators of SOM lability

278

279 We first assessed the relationship between C release rates in incubation experiments and widely
280 available physico-chemical parameters in samples from soil carbon inventories carried out
281 throughout the northern permafrost region. The latter include dry bulk density (DBD), C content as a
282 percentage of dry sample weight (%C), and carbon to nitrogen weight ratios (C/N). In recent studies
283 dealing with incubation of soil samples from the northern permafrost region, %C and C/N of soil
284 samples were highlighted as best parameters to predict C release (Elberling et al., 2013; Schädel et
285 al., 2013). DBD was highlighted as a useful proxy in the recent synthesis of PAGE21 incubation



286 studies presented in Faucherre et al. (2018). All three parameters are significantly (anti-)correlated
287 with each other in the four different incubation experiments (Table 1 and Fig. S1). This can be
288 expected, since organically enriched topsoil samples have low DBD, high %C and high C/N values
289 compared to mineral layer soil samples. Also deeper soil samples, C-enriched through the process of
290 cryoturbation (Bockheim, 2007), have generally relatively low DBD, high %C and high C/N values
291 compared to adjacent mineral soil samples (e.g. Hugelius et al., 2010; Palmtag et al., 2015).

292

293 Table 1. R^2 values of cross correlations between three geochemical parameters for all samples in the
294 PAGE21 and three CryoCarb incubation experiments (all significant, $p < 0.05$). For regression
295 models see Fig. S1.

296

297 All three considered geochemical parameters are significantly (anti-)correlated with measured C
298 release rates in the four different incubation experiments. Lower DBD, higher %C and higher C/N
299 values are associated with higher C-CO₂ production per gdw of the samples (Table 2 and Fig. S2).
300 Of the three parameters, DBD explains most of the observed variability in C release in two
301 experiments, whereas C/N shows highest R^2 values in the other two experiments.

302

303 Table 2. R^2 values of regressions between three geochemical parameters and $\mu\text{gC-CO}_2$ production
304 per gram dry weight for all samples in the PAGE21 and the three CryoCarb incubation
305 experiments (all significant, $p < 0.05$). For regression models see Fig. S2.

306

307 3.2. Partitioning of the datasets based on landscape unit classes

308

309 Our results show a significant relationship between $\mu\text{gC-CO}_2$ production per gdw as a function of
310 %C of the soil sample for the full datasets in each of the four incubation experiments (Fig. S2).
311 However, less than 50 % of the variability is explained by this relationship, which implies that it has
312 limited usefulness to predict C release based on %C of the samples only (Table 2). In this section we
313 analyze whether a grouping of samples according to landscape unit classes can disentangle some of
314 the observed variability.

315 Figure 2 shows the significant relationships between C release rates and %C in the samples for
316 the full datasets in the PAGE21 (measured on day 343 of incubation) and CryoCarb 1-Kolyma
317 (measured over the first four days of incubation) experiments. A first observation is that C release
318 rates per gdw are c. 15 times lower in the longer-term PAGE21 experiment compared to the short-
319 term CryoCarb 1-Kolyma experiment. Both experiments show a large range in C release, particularly
320 at medium to high %C values. Figure 3 shows the same two experiments and data points, but
321 grouped according to major landscape unit classes. For the sake of simplicity, we apply linear
322 regressions with intercept zero to all groups. The linear regression for the full data set is provided as
323 reference, but it should be noted that its slope is partly determined by the number of samples in each
324 of the recognized landscape units. These are identified by different colors and symbols that have
325 been consistently applied in Figs. 3-4 and S3-S5.

326

327 Figure 2. $\mu\text{gC-CO}_2$ production per gram dry weight as a function of %C of the sample for the full
328 datasets in the (a) PAGE21 (top panel) and (b) CryoCarb 1-Kolyma (lower panel) incubation
329 experiments (both regressions significant, $p < 0.05$).

330

331 In the PAGE21 dataset (Fig. 3a), the soils developed into alluvial and eolian deposits and in
332 peaty wetlands all show similar and relatively high SOM lability. Mineral soils show intermediate



333 values, whereas the peat deposits display low SOM lability (when considering %C values). All
334 regressions are significant, except for ‘peat deposits’ due to very high variability in three surface peat
335 samples (but see Fig. 4d). In the CryoCarb 1-Kolyma data set (Fig. 3b), alluvial and eolian
336 soils/deposits show the highest SOM lability, followed by mineral soils. In this case, peaty wetlands
337 show a slightly lower lability than mineral soils/deposits but still considerably higher than peatlands.
338 This clear dichotomy in the SOM lability of mineral soils (including peaty wetlands) and peat
339 deposits is also apparent from the CryoCarb 2-Taymyr and CryoCarb 3-Seida results even though not
340 all landscape classes are represented in those experiments (Fig. S3). The explanatory power of the
341 regressions (R^2 values) in the peatland class is generally lower than that in the mineral soil/deposit
342 classes. These statistics are, however, greatly improved when removing the surface peat samples
343 from the analyses (not shown), which display very high variability.

344

345 Figure 3. $\mu\text{gC-CO}_2$ production per gram dry weight as a function of %C of the sample for the
346 different landscape classes in the longer-term PAGE21 (a, top panel) and short-term CryoCarb
347 1-Kolyma (b, lower panel) incubation experiments: Alluvial class (red line and diamonds);
348 Eolian class (blue line and triangles); Mineral class (brown line and squares); Peaty wetland
349 class (dark green line and circles); Peatland class (light green line and circles). All regressions
350 significant, $p < 0.05$, except for the PAGE21 peatland class (n.s.).

351

352 Linear regression analyses between C- CO_2 production per gdw and C/N ratios for all four
353 experiments (Fig. S4) show small deviations from the above patterns but generally maintain the clear
354 difference between ‘peat deposits’ and the remaining landscape units. However, peat deposits with
355 low C/N values (≤ 20) seem to decompose at similar rates as SOM in mineral soils and deposits with
356 similar C/N ratios. R^2 values for the landscape classes are generally lower than in regressions against
357 %C and regression lines at low C release tend to converge to C/N values of 8-12, which are typical
358 for microbial decomposer biomass suggesting only slow internal cycling of remaining SOM
359 (Zechmeister-Boltenstern et al., 2015).

360 The PAGE21 dataset with C- CO_2 production rates expressed per gC as a function of %C of the
361 soil sample also shows similar results, however, with generally lower R^2 and sometimes non-
362 significant regressions (Fig. S5a). The same patterns are also noted when expressing C release as a
363 function of soil volume (cm^3), however, R^2 values are generally even lower and more often non-
364 significant (Fig. S5b).

365

366 3.3. Further subdivision of landscape unit classes in the PAGE21 dataset

367

368 In Fig. 4, landscape unit classes in the PAGE21 dataset have been further subdivided and different
369 functions (second order polynomial or exponential) providing better fits have been applied. The
370 eolian class is subdivided into actively accumulating deposits (Adventdalen) and Holocene soils
371 formed into Pleistocene Yedoma parent materials (Lena Delta), and specifically identifies buried C-
372 enriched samples (Fig. 4a). Alluvial deposits are separated into profiles from active and pre-recent
373 floodplains (multiple study areas), again separating samples from deeper C-enriched buried layers
374 and cryoturbated pockets (Fig. 4b). Mineral soils are separated into active colluviation sheets
375 (mountain slopes on Svalbard) and other mineral soils (multiple study areas), highlighting the one
376 buried C-enriched sample found in this class (Fig. 4c). Generally speaking, a second order
377 polynomial (intercept zero) provides the best fit and has been applied for the sake of uniformity to all
378 described subclasses. All these three datasets have in common that the subclasses with active surface
379 accumulation/movement have topsoil samples that show relatively low C content due to the
380 continuous admixture of minerogenic materials. At the same time, these all show the highest C- CO_2



381 production per gdw (when considering %C). Furthermore, the second order polynomial regressions
382 of all subclasses (except for buried C-enriched samples) suggest that the topsoil samples are
383 particularly labile suggesting the presence of a ‘fast’ SOM pool in the recently deposited plant litter.
384 Deeper C-enriched material shows relatively low lability and does not show rapidly increasing
385 lability at higher %C values.

386 Figure 4d compares the SOM lability in peat deposits (fens and bogs in Stordalen Mire) and
387 peaty wetland profiles (multiple study areas), adding for comparison the results from the previously
388 described deeper C-enriched buried layers and cryoturbated pockets in mineral soils (see Figs. 4a-c).
389 In this case, exponential functions best describe observed trends, pointing to very high lability of
390 surface peat(y) samples. The thin peat layers in peaty wetlands have relatively low %C values
391 pointing to admixture of minerogenic materials. The SOM in these profiles show relatively high C-
392 CO₂ production per gdw compared to ‘true’ peat samples (when considering %C). Compared to the
393 non-significant linear regression for all peat samples shown in Fig. 3a, exponential regressions for
394 the peatland class as a whole as well as for fens and bogs separately are statistically significant.
395 Particularly in fen peat, this regression is able to capture some very high C release values of two
396 surface peat samples (corresponding to graminoid-derived plant litter). Deeper C-enriched material
397 in mineral soils displays only slightly higher SOM lability compared to the mineral subsoil
398 underlying peat deposits. It is important to bear in mind that the total number of peat samples from
399 Stordalen Mire is limited (n=13) and that results cannot be compared directly to adjacent mineral soil
400 profiles because field sampling in that particular study area focused solely on the peatland area.

401

402 Figure 4. $\mu\text{gC-CO}_2$ production per gram dry weight as a function of %C of the sample for different
403 landscape classes and their subdivisions in the PAGE21 incubation experiment. (a) Eolian class
404 separated into actively accumulating deposit (light blue), Holocene soil formation into
405 Pleistocene Yedoma parent materials (dark blue) and buried C-enriched samples (pink); (b)
406 Alluvial class separated into active floodplain (rose), Holocene soil formation into pre-recent
407 floodplain deposits (red) and buried C-enriched samples (pink); (c) Mineral class separated into
408 active colluviation sheet (light brown), other mineral soils (dark brown) and buried C-enriched
409 samples (pink); (d) wetland class separated into wetlands with thin peat layers (green), fens
410 (light green) and bogs (dark green) with deep peat deposits and, for comparison, buried C-
411 enriched samples in mineral soils (pink). The hatched line represents the regression for all true
412 peatland samples (fens and bogs) together. C-release from one surface peat sample (green-
413 orange) in the margin of a peatland is also indicated, but not included in the regressions. All
414 regressions are significant ($p < 0.05$).

415

416 3.4. C-enriched cryoturbated and Pleistocene Yedoma samples in the CryoCarb 1-Kolyma dataset

417

418 In the PAGE21 incubation each profile included only one sample from the mineral soil in the middle
419 of the active layer and one sample from the upper permafrost layer. Thus, the selection of samples
420 was based on depth-specific criteria. As a result, the number of samples from deeper C-enriched
421 buried layers and cryoturbated pockets is limited (n=13). In the CryoCarb 1-Kolyma experiment
422 samples from entire profiles were incubated and the number of deeper C-enriched samples in the
423 mineral soil horizons is much larger. Figure 5a compares the C-CO₂ production per gdw from
424 organically-enriched topsoil and mineral soil samples not affected by C-enrichment with that in
425 deeper C-enriched cryoturbated samples in tundra upland profiles. For the sake of clarity, only those
426 cryoturbated samples which are C-enriched by at least twice the adjacent mineral soil %C
427 background values are included (n=22). The results from this much more narrowly defined dataset
428 are similar to those presented for the PAGE21 experiment, i.e. SOM in deeper C-enriched
429 cryoturbated samples is less labile than in organically-enriched topsoil samples with similar %C.



430 The PAGE21 experiment does not include any samples from Pleistocene Yedoma deposits. In
431 contrast, the CryoCarb 1-Kolyma dataset includes samples from two Yedoma exposures along river
432 and thermokarst lake margins. The material was collected from perennially frozen Yedoma deposit
433 as well as from thawed out sections of the exposures. C-release from these samples are presented in
434 Fig. 5b, which for comparison also shows low %C samples from the upper permafrost horizon in
435 Holocene tundra soils formed into Yedoma parent materials, mineral subsoil samples beneath peat
436 deposits and samples from deeper C-enriched cryoturbated samples. The C-CO₂ production per gdw
437 of Pleistocene Yedoma is lower than that of permafrost horizon samples in Holocene soils, but
438 somewhat higher to that of samples from mineral subsoil beneath peat and deeper C-enriched
439 samples (when considering %C). Furthermore, the SOM lability of thawed out deposits is somewhat
440 lower than that of the intact permafrost Yedoma material.

441

442 Figure 5. $\mu\text{gC-CO}_2$ production per gram dry weight as a function of %C of the sample in the
443 CryoCarb 1-Kolyma incubation experiment for (a) deeper C-enriched samples (pink line and
444 triangles), compared to organically enriched topsoil and mineral soil samples not affected by C-
445 enrichment in Holocene tundra upland profiles (blue line and triangles), and for (b) perennially
446 frozen Pleistocene Yedoma samples (black line and triangles) and thawed out Pleistocene
447 Yedoma samples (red line and triangles), compared to upper permafrost layer samples in
448 Holocene tundra upland soils (blue line and triangles), mineral subsoil samples beneath peat
449 deposits (green line and circles, showing start of regression line) and buried C-enriched samples
450 (pink line and triangles, showing start of regression line). All regressions (power fit) are
451 significant ($p < 0.05$).

452

453 3.5. Relative lability ranking of SOM landscape unit classes

454

455 Table 3a shows the slopes of the linear regressions (intercept zero) between C-CO₂ production per
456 gdw and %C of samples for the different landscape unit classes in all four incubation experiments.
457 From these results it is clear that results from the four experiments cannot be compared directly in
458 quantitative terms. To facilitate comparison across experiments the results were therefore normalized
459 to the lowland mineral soil class, which consistently showed intermediate SOM labilities. Table 3b
460 shows the normalized regression slopes (with the slope for mineral soils set to 1), and their mean and
461 standard deviation (when the landscape class is represented in more than one incubation experiment).
462 This approach confirms the previous results that peat deposits and deeper C-enriched samples in
463 mineral soils consistently show very low relative lability, whereas areas with recent mineral sediment
464 accumulation (in active floodplains and recent eolian deposits) display generally somewhat higher
465 SOM lability (when considering %C). Pleistocene Yedoma deposits, only represented in one
466 incubation experiment, also display relative low SOM lability.

467

468 Table 3. (a) Slopes of linear regressions (intercept zero) between %C and C-CO₂ production per gdw
469 in samples of the different landscape classes in the four experiments; (b) Normalized slopes of
470 linear regressions between %C and C-CO₂ production per gdw for samples in the different
471 landscape classes in the four experiments (slope of mineral soils in lowland settings set to 1).

472

473 3.6. SOM lability based on soil horizon criteria

474

475 We also tested SOM lability in samples grouped according to soil horizon criteria, with special
476 attention to those horizon classes that can be linked to the specific landscape units that show low
477 relative SOM lability (C-enriched pockets for Turbels, peat samples for Histels and loess samples for



478 Pleistocene Yedoma). This approach yielded classes with data distributions that are much better
479 constrained in terms of %C values.

480 For the mineral soils in the PAGE21 incubation experiment, we differentiated between the
481 topsoil organic layer, the active layer mineral soil, the permafrost layer mineral soil, and C-enriched
482 pockets in both active layer and permafrost layer. Samples from topsoil organic layer, the active
483 layer mineral soil and the permafrost layer mineral soil from profiles formed in Late Holocene loess
484 deposits in Adventdalen (Svalbard) are considered separately, as are the active layer peat samples
485 from Stordalen Mire (N Sweden). A similar grouping has been made for mineral soils in the
486 CryoCarb 1-Kolyma experiment. In this case, Pleistocene Yedoma loess samples (both frozen and
487 thawed) are considered separately. Peat samples are much better represented in the CryoCarb 1-
488 Kolyma than PAGE21 experiment, and are subdivided into samples from thin peat layers in the
489 active layer of peaty wetlands (Histis Gelisols), as well as samples from the active layer and
490 permafrost layer of deep peat deposits (Histels).

491 In this analysis we focus on C-CO₂ production per gC to take into account large differences in
492 %C between soil horizon classes (see Fig. S6). The main difference between the two experiments is
493 the much lower %C values of the topsoil organic class in the PAGE21 incubation, which can be
494 explained by a greater surface admixture of minerogenic material in alluvial (Lena Delta), eolian and
495 mountainous areas (Svalbard). In contrast, the predominant lowland setting of the CryoCarb 1-
496 Kolyma study area is characterized by soils with thicker, more C-rich, topsoil organic layers.

497 Figure 6 shows C-CO₂ production per gC in the soil horizon groups of the longer term PAGE21
498 and short-term CryoCarb 1-Kolyma experiments. Results of the Mann-Whitney paired tests for both
499 these experiments are shown in Table 4. PAGE21 classes show fewer statistically significant
500 differences than in the CryoCarb 1-Kolyma experiment, which can at least partly be ascribed to
501 smaller sample sizes. The number of samples in the PAGE21 incubation for C-enriched pockets in
502 the active layer (n=3) and for peat (n=6) are particularly low.

503

504 Figure 6. $\mu\text{gC-CO}_2$ production per gram carbon in samples of (a) the PAGE21 and (b) the CryoCarb
505 1-Kolyma incubation experiments, grouped according to soil horizon criteria. Abbreviations:
506 AL-OL = Active layer topsoil organics; AL-Min = Active layer mineral; AL-Ce = Active layer
507 C-enriched; P-Min = Permafrost layer mineral; P-Ce = Permafrost layer C-enriched; AL-Pty =
508 Active layer thin peat (CryoCarb 1-Kolyma experiment only); AL-Pt = Active layer peat; P-Pt =
509 Permafrost layer peat (CryoCarb 1-Kolyma experiment only); AL-Lss OL = Active layer topsoil
510 organics in Late Holocene loess deposits (PAGE21 experiment only); AL-Lss Min = Active
511 layer mineral in Late Holocene loess deposits (PAGE21 experiment only); P-Lss Min =
512 Permafrost layer mineral in Late Holocene loess deposits (PAGE21 experiment only); P-Yed =
513 Permafrost Pleistocene Yedoma deposits (CryoCarb 1-Kolyma experiment only); Th-Yed =
514 Thawed out Pleistocene Yedoma deposits (CryoCarb 1-Kolyma experiment only). Box-whisker
515 plots show mean and standard deviation (in red) and median, first and third quartiles and
516 min/max values (in black), for the different soil horizon groups.

517

518 Table 4. p Values of Mann-Whitney paired tests of $\mu\text{gC-CO}_2$ production per gram carbon for soil
519 horizon groups in (a) the PAGE21 and (b) the CryoCarb 1-Kolyma incubation experiments.
520 Abbreviations as in Fig. 6. Differences are considered significant when $p < 0.05$.

521

522 The C release rates in topsoil organic samples from the actively accumulating Holocene loess
523 soils are significantly higher than those in topsoil organic samples from the remaining PAGE21
524 mineral soils (Fig. 6a and Table 4a). Both topsoil organic classes show significantly higher rates than
525 all mineral soil and peat classes. Peat samples have the lowest mean and median C release rates from



526 all these classes but only the rates from permafrost layer mineral soil and C-enriched pocket samples
527 are significantly higher. Both mean and median C release rates from active layer and permafrost
528 layer C-enriched pockets are somewhat lower (but not significantly different) than those from
529 adjacent, non C-enriched, mineral soil samples.

530 C release rates in the soil horizon classes from the CryoCarb 1-Kolyma experiment show
531 similarities, but also some differences to those observed in the PAGE21 experiment. Absolute C
532 release rates per gC are more than an order of magnitude higher in the CryoCarb 1-Kolyma
533 experiment (measured as a mean release over the first four days of incubation) compared to those in
534 the PAGE21 experiment (measured at day 343). Another important difference is that C release rates
535 per gC in the short-term CryoCarb 1-Kolyma incubation do not differ significantly between the
536 topsoil organic class and the active layer and permafrost layer mineral soil classes, which we ascribe
537 to the presence of a highly labile C pool (e.g. DOC, plant roots) in the mineral soil layers that is
538 quickly decomposed (see Weiss et al., 2016; Faucherre et al., 2018). However, rates from active
539 layer and permafrost layer C-enriched pockets are significantly lower than those from adjacent, non
540 C-enriched, mineral soil samples. Both active layer and permafrost layer peat samples show
541 significantly lower C release rates than all other classes, with active layer peat samples having
542 significantly higher rates than permafrost layer peat samples. Samples from the Pleistocene Yedoma
543 loess ‘frozen’ and ‘thawed’ classes display significantly lower C release rates per gC than those in
544 the topsoil organic layer, active layer and permafrost layer mineral soil classes, but significantly
545 higher rates than those in the peat classes. The two Yedoma classes do not differ significantly from
546 each other, the active layer and permafrost layer C-enriched pocket classes, nor the peaty wetland
547 class.

548

549 4. Discussion

550

551 The analysis and comparison of results in the PAGE21 and CryoCarb 1-Kolyma incubations show
552 consistent trends in C-CO₂ production rates as a function of simple soil geochemical parameters in
553 both the full datasets as well as in the grouping of samples according to landscape classes. However,
554 it is not possible to directly compare these two very different laboratory experiments quantitatively.
555 The varying field collection techniques, field storage, transport and laboratory storage, pretreatment,
556 experimental setup and time of measurement after start of incubations have a clear effect on the
557 magnitude of the observed C-CO₂ production rates. The same methods were applied to all samples
558 from all study areas in the PAGE21 experiment, but these differed markedly from those applied in
559 the CryoCarb setup and even between the three individual CryoCarb experiments (e.g., addition of
560 different ‘local’ microbial decomposer inoculi to rewetted samples).

561 In quantitative terms, C-CO₂ production rates per gdw measured over the first 4 days in the
562 CryoCarb 1-Kolyma samples incubated at 12 °C are about 15 times higher than those after about one
563 year in the PAGE21 samples incubated at 5 °C (see Fig. 2). Similarly, C-CO₂ production rates per gC
564 are also more than an order of magnitude higher in the short-term CryoCarb-Kolyma 1 than the
565 longer term PAGE21 incubation (see Fig. 6). Upper permafrost mineral soil samples (<3 %C) from
566 Kylatyk in NE Siberia, incubated at 2 °C directly after field collection and thawing (measurement
567 after 20-30 hr, following 3 days of pre-incubation), show median C release rates of c. 750 μgC-CO₂
568 gC⁻¹ d⁻¹ (Weiss et al., 2016), compared to c. 1750 μgC-CO₂ gC⁻¹ d⁻¹ in the same class of CryoCarb 1-
569 Kolyma samples. Median C release rates in upper permafrost mineral soil samples of the PAGE21
570 experiment (Faucherre et al., 2018) decrease from c. 170 on day 8 to c. 35 μgC-CO₂ gC⁻¹ d⁻¹ on day
571 343 since start of incubation. It is obvious from these results that there is a rapid decline in C release
572 rates over time of incubation. Longer incubation experiments (up to 12 years) have shown that the
573 overall rate of C loss decreases almost exponentially over time (Elberling et al., 2013). However,
574 even when laboratory incubation setups and time of measurement are similar, large differences can



575 occur in C release rates. For instance, peat samples in the CryoCarb 1-Kolyma incubation display
576 about twice the C-CO₂ production rates per gdw than those observed in the CryoCarb 3-Seida
577 incubation (Figs. 3b and S3b).

578 Nonetheless, a comparison of C-CO₂ production rates per gdw for landscape unit classes in
579 terms of relative SOM lability provided useful and robust results. These classes were implemented to
580 allow upscaling of results to the northern permafrost region. They reflect main Gelisol (and non-
581 Gelisol) soil suborders and deeper Quaternary deposits to permit direct comparison with the size and
582 geographic distribution of these different SOC pools (Tarnocai et al., 2009; Hugelius et al., 2014).
583 Samples from mineral soil profiles, including wetland deposits with a thin peat(y) surface layer,
584 display high relative SOM lability compared to peat deposits, deep C-enriched buried or cryoturbated
585 samples and Pleistocene Yedoma deposits (when considering %C of the incubated sample). These
586 results are confirmed by the more stringent statistical analysis of samples grouped into soil horizon
587 classes. Peat deposit, C-enriched pocket and Yedoma deposit samples show significantly lower C-
588 CO₂ production rates per gC than topsoil organics and mineral layer samples (Cryo-Carb-1-Kolyma
589 experiment). The same trends are observed in the incubation experiment of upper permafrost samples
590 from Kytalyk, reported by Weiss et al. (2016). C-enriched pockets (3-10 %C) showed lower C-CO₂
591 production rates per gC than mineral soil samples (<3 %C), while a buried peat sample (c. 40 %C)
592 displayed a very low C-CO₂ production rate per gC. The PAGE21 experiment also revealed that peat
593 samples mineralized a smaller fraction of C over the one year of incubation compared to mineral soil
594 samples (Faucherre et al., 2018).

595 A further subdivision of landscape classes and more careful analysis of incubation results in the
596 PAGE21 experiment provide additional useful insights. For example, separation of eolian deposits
597 into actively accumulating deposits during the Late Holocene (Adventdalen) and Holocene soils
598 formed into Pleistocene Yedoma parent materials (Lena Delta) showed clear differences in C release
599 rates per gdw (when considering %C), with the former displaying a higher SOM lability in topsoil
600 organic samples (see Fig. 4a). The topsoil organic samples from the actively accumulating eolian
601 deposits in Adventdalen also displayed significantly higher C release rates per gC than all other
602 topsoil organic, mineral layer and peat(y) horizon classes (see Table 4a). Separation of alluvial
603 deposits into active floodplain deposits and Holocene soils formed in pre-recent river terraces and of
604 mineral soils into active colluviation sheets (mountain slopes on Svalbard) and other mineral soils
605 (multiple study areas) showed similar trends in SOM lability (see Fig. 4b-c). These results suggest
606 that admixture of minerogenic material in topsoil organics of actively accumulating eolian, alluvial
607 and colluvial deposits promotes SOM decomposition. Peaty wetland deposits display much higher C
608 release rates per gdw (when considering %C) than peatland deposits (see Fig. 4d). These two
609 landscape classes are poorly represented in the PAGE21 experiment, but a statistical test of C release
610 rates per gC in these peat(y) soil horizon classes of the CryoCarb 1-Kolyma incubation confirms this
611 difference (see Table 4b). This is interesting because even though wetlands with a thin peat layer do
612 not have particularly high C stocks, they can be important sources of methane (CH₄) to the
613 atmosphere (Olefeldt et al., 2013). These further subdivisions into landscape subclasses are of
614 limited use for upscaling purposes because they are not considered explicitly in any available
615 geographic database for the northern permafrost region.

616 The relatively low lability in the peatland class is surprising. The low DBD, high %C and high
617 C/N of peat are normally associated with a relatively low degree of decomposition. This, in turn, is
618 the result of environmental factors such as anaerobic and/or permafrost conditions that largely inhibit
619 SOM decay (Davidson and Janssens, 2006). One could expect that this less decomposed material
620 would show high lability following thawing and warming, but our results point to the opposite. This
621 is particularly surprising when considering the setup of the CryoCarb experiments, in which a slush
622 of rewetted material inoculated with microbial decomposers was incubated at 12 °C. The CryoCarb
623 experiments are very short assays (4 days), but the longer term PAGE21 experiment (measured after



624 roughly one year) provides similar results. As previously suggested by Capek et al. (2015), also
625 SOM from deeper C-enriched buried layers and cryoturbated pockets show relatively low lability
626 when compared to organically-enriched topsoil and mineral layer samples not affected by C-
627 enrichment in all incubation experiments. To these two categories of samples can be added
628 Pleistocene Yedoma deposits, which despite incorporation of relative fresh plant root material caused
629 by syngenetic permafrost aggradation, also display low relative SOM lability. This implies that SOM
630 in three of the major SOC pools in the northern permafrost region, i.e. deeper peat deposits in
631 Histels/Histosols, deeper C-enriched material in Turbels and Pleistocene Yedoma deposits, display a
632 high level of resistance to decomposition. The reason why this relatively undecomposed material
633 displays low lability remains unclear. One reason could be that the decomposer community needs
634 time to adapt to the new environmental conditions following thawing/warming, another one that
635 there is a simple mismatch between the microbial community adapted to decompose relatively
636 undecomposed organic material and the physico-chemical environment (e.g., higher bulk density)
637 prevailing in (thawed out) deeper soil horizons (Gittel et al., 2013; Schnecker et al., 2014). In the
638 case of peat deposits, it should also be considered if this resistance to decomposition is an evolved
639 'biochemical trait' in peat-forming species that maintains their favored habitat, similar to the role of
640 *Sphagnum* anatomy (hyaline cells), physiology (acidification) and cell wall chemistry (phenolic
641 compounds) in sustaining moist and acid surface conditions, and inhibiting peat decomposition
642 (Clymo and Hayward, 1982). Furthermore, the generally high C/N ratios of peat provide a poor
643 substrate quality to the decomposer community (Bader et al., 2018).

644 An important consideration is if the consistent differences in relative SOM lability of landscape
645 and soil horizon classes observed in our incubation experiments will be maintained over periods of
646 decades to centuries of projected warming and thawing. Very short-term incubations, such as in the
647 CryoCarb setup (four days), might register the initial decomposition of highly labile SOM
648 components, such as microbial necromass, simple molecules (e.g., sugars or amino acids), low
649 molecular-weight DOC, etc., or might not provide enough time for an adaptation of the microbial
650 decomposer community to new environmental settings (Weiss et al., 2016; Weiss and Kaal, 2018).
651 On the other hand, in longer incubation experiments such as in the PAGE21 experiment (one year),
652 the conditions in the incubated samples become gradually more artificial compared to field
653 conditions. Specifically, microbes in long-term incubations become increasingly C limited, as no
654 new C input by plants occur, whereas inorganic nutrients, such as nitrate or ammonium accumulate
655 to unphysiological levels. Care, therefore, should be taken when extrapolating our results over longer
656 time frames if no corroborating field evidence for longer term decay rates can be obtained (e.g.
657 Kuhry and Vitt, 1996; Schuur et al., 2009).

658

659 5. Conclusions

660

661 The PAGE21 and CryoCarb incubation experiments confirm results from previous studies that
662 simple geochemical parameters such as DBD, %C and C/N can provide a good indication of SOM
663 lability in soils and deposits of the northern permafrost region (Elberling et al., 2013; Schädel et al.,
664 2013; Faucherre et al., 2018.). In our analyses we have focused on %C of the sample since it is the
665 most widely available of the three investigated geochemical parameters. Furthermore, %C is less
666 sensitive than C/N to botanical origin of the plant litter and, in contrast to DBD, not dependent on
667 ground compaction or volume of excess ground ice.

668 When considering the full datasets of the four experiments, our regressions of C release as a
669 function of %C were statistically significant but explained less than 50 % of the observed variability.
670 Subsequently, we investigated whether a further division of samples into predefined landscape unit
671 classes would better constrain the observed relationships. In defining these classes, we applied a
672 scheme that could easily be used for spatial upscaling to northern circumpolar levels. We adopted the



673 main Gelisol suborders (Histels, Turbels and Orthels), non-permafrost Histosols and mineral soils,
674 and types of deeper Quaternary (deltaic/floodplain and eolian/Yedoma) deposits used in the NCSCD
675 and related products to estimate the total SOC pool in the northern permafrost region (Tarnocai et al.,
676 2009; Strauss et al., 2013; Hugelius et al., 2014). We conclude that these landscape classes better
677 constrain observed variability in the relationships and that the relative SOM lability rankings of these
678 classes were consistent among all four incubation experiments, for both regressions against %C and
679 C/N (all four experiments), and for regressions of %C against different units of C-CO₂ production
680 'per gram dry weight', 'per gram C' and 'per cm³' (PAGE21 dataset). Our results based on full
681 profiles indicate that C-CO₂ production rates per gdw decrease in the order Late Holocene eolian >
682 alluvial and mineral upland (including peaty wetlands) > Pleistocene Yedoma > C-enriched pockets
683 > peat, with lowest C release rates observed in peat deposits (when considering %C). These results
684 are corroborated by statistical analysis of C release rates per gC for samples grouped according to
685 soil horizon criteria (PAGE21 and CryoCarb 1-Kolyma datasets).

686 An important conclusion from these results is that purportedly more undecomposed SOM, such
687 as in peat deposits (Histels and Histosols), C-enriched cryoturbated samples (Turbels), and
688 Pleistocene Yedoma deposits, does not seem to imply higher SOM lability. These three SOC pools
689 together represent ≥50 % of the reported SOC storage in the northern permafrost region (Hugelius et
690 al., 2014; Palmtag and Kuhry, 2018). Consequently, there is an urgent need for further research to
691 understand these results in order to better constrain the thawing permafrost carbon feedback on
692 global warming.

693

694 6. Data availability

695

696 The soil geochemical data and incubation results presented in this paper are available upon request
697 from PK (peter.kuhry@natgeo.su.se). For full PAGE21 incubation data, please contact BE
698 (be@ign.ku.dk). For full CryoCarb incubation data, please contact JB (jiri.barta@prf.jcu.cz).

699

700 7. Author contribution

701

702 PK developed the initial concept for the study. All authors contributed with the collection of soil
703 profiles at various sites. The PAGE21 incubation experiment was planned and conducted at
704 CENPERM (University of Copenhagen) by SF and BE, whereas the CryoCARB incubation
705 experiments were carried out at the University of South Bohemia (Ceske Budejovice) under
706 guidance of HS and JB. PK performed all statistical analyses, in cooperation with GH. All co-authors
707 contributed to the writing of the manuscript, including its discussion section.

708

709 8. Competing interests

710

711 The authors declare that they have no conflict of interest.

712

713 9. Acknowledgments

714

715 Collection and laboratory analyses for Svalbard (Adventdalen and Ny Ålesund), Stordalen Mire and
716 Lena Delta samples were supported by the EU-FP7 PAGE21 project (grant agreement no 282700).
717 Lower Kolyma and Taymyr Peninsula samples were collected and incubated in the framework of the
718 ESF-CryoCarb project, with support from the Swedish Research Council (VR to Kuhry), the



719 Austrian Science Fund (FWF I370-B17 to Richter), the Czech Science Foundation (Project 16-
720 18453S to Barta) and the Czech Soil-Water Research Infrastructure (MEYS CZ grants LM2015075
721 and EF16-013/0001782 to Šantrůčková). Seida samples were originally collected in the framework
722 of the EU-FP6 Carbo-North project (contract 036993). Gustaf Hugelius acknowledges a Swedish
723 Research Council Marie Skłodowska Curie International Career Grant. We thank Christian Jungner
724 Jørgensen (University of Copenhagen) for guidance and assistance in the PAGE21 incubation
725 experiment. Kateřina Diáková is acknowledged for the collection of the soil inoculi in Seida. The
726 Seida samples were subsequently incubated at the University of South Bohemia. We are most
727 grateful to Nikolai Lashchinskiy (Siberian Branch of the Russian Academy of Sciences,
728 Novosibirsk) and Nikolaos Lampiris, Juri Palmtag, Nathalie Pluchon, Justine Ramage, Matthias
729 Siewert and Martin Wik (all Stockholm University), for help in sample collection. We would also
730 like to thank Magarethe Watzka (University of Vienna) for elemental analyses of soil samples.
731 Zhanna Kuhrij is acknowledged for the preparation of Figs. 6 and S6.

732

733 10. References

734

- 735 Bader, C., Müller, M., Schulin, R., and Leifeld, J.: Peat decomposability in managed organic soils in
736 relation to land use, organic matter composition and temperature, *Biogeosciences* 15, 703–719,
737 <https://doi.org/10.5194/bg-15-703-2018>, 2018.
- 738 Bockheim, J. G.: Importance of cryoturbation in redistributing organic carbon in permafrost-affected
739 soils, *Soil Sci. Soc. Am. J.* 71(4), 1335–1342, <https://doi.org/10.2136/sssaj2006.0414N>, 2007.
- 740 Brown, J., Ferrians Jr., O. J., Heginbottom, J. A., and Melnikov, E. S.: Circum-Arctic map of
741 permafrost and ground-ice conditions, 1 : 10 000 000, Map CP-45, United States Geological
742 Survey, International Permafrost Association, Washington, D. C., 1997.
- 743 Burke, E. J., Hartley, I. P., and Jones, C. D.: Uncertainties in the global temperature change caused
744 by carbon release from permafrost thawing, *The Cryosphere*, 6, 1063–1076,
745 <https://doi.org/10.5194/tc-6-1063-2012>, 2012.
- 746 Čapek, P., Diáková, K., Dickopp, J. E., Bárta, J., Wild, B., Schneckner, J., and Hugelius, G.: The
747 effect of warming on the vulnerability of subducted organic carbon in arctic soils, *Soil Biol.*
748 *Biochem.*, 90, 19–29, <https://doi.org/10.1016/j.soilbio.2015.07.013>, 2015.
- 749 Ciais, P.: A geoscientist is astounded by Earth’s huge frozen carbon deposits, *Nature*, 462, 393,
750 <https://doi.org/10.1038/462393e>, 2009.
- 751 Clymo, R. S. and Hayward, P. M.: The Ecology of *Sphagnum*, in: Smith, A. J. E. (ed). *Bryophyte*
752 *Ecology*. 540, 229–289, https://doi.org/10.1007/978-94-009-5891-3_8, 1982.
- 753 Davidson, E. A. and Janssens, I. A.: Temperature sensitivity of soil carbon decomposition and
754 feedbacks to climate change, *Nature*, 440, 165–173, <https://doi.org/10.1038/nature04514>, 2006.
- 755 Elberling, B., Michelsen, A., Schädel, C., Schuur, E. A., Christiansen, H. H., Berg, L., Tamstorf, M.
756 P., and Sigsgaard, C.: Long-term CO₂ production following permafrost thaw, *Nature Climate*
757 *Change*, 3(10), 890–894, <https://doi.org/10.1038/nclimate1955>, 2013.
- 758 Faucherre, S., Jørgensen, C. J., Blok, D., Weiss, N., Siewert, M. B., Bang-Andreasen, T., Hugelius,
759 G., Kuhry, P., and Elberling, B.: Short and long-term controls on active layer and permafrost
760 carbon turnover across the Arctic, *J. Geophys. Res.--Biogeosciences.*, 123(2), 372–390.,
761 <https://doi.org/10.1002/2017JG004069>, 2018.
- 762 Fierer, N. and Schimel, J. P.: A proposed mechanism for the pulse in carbon dioxide production
763 commonly observed following the rapid rewetting of a dry soil. *Soil Sci. Soc. Am. J.*, 67(3),
764 798–805, <https://doi.org/10.2136/sssaj2003.0798>, 2003.



- 765 Franzluebbers, A. J., Haney, R. L., Honeycutt, C. W., Schomberg, H. H., and Hons, F. M.: Flush of
766 carbon dioxide following rewetting of dried soil relates to active organic pools, *Soil Sci. Soc.*
767 *Am. J.*, 64(2), 613–623, <https://doi.org/10.2136/sssaj2000.642613x>, 2000.
- 768 Gentsch, N., Mikutta, R., Alves, R. J. E., Barta, J., Čapek, P., Gittel, A., Hugelius, G., Kuhry, P.,
769 Lashchinskiy, N., Palmtag, J., Richter, A., Šantrůčková, H., Schneckner, J., Shibistova, O., Urich,
770 T., Wild, B., and Guggenberger, G.: Storage and transformation of organic matter fractions in
771 cryoturbated permafrost soils across the Siberian Arctic, *Biogeosciences*, 12(14): 4525–4542,
772 <https://doi.org/10.5194/bg-12-4525-2015>, 2015.
- 773 Gittel, A., Bárta, J., Kohoutová, I., Mikutta, R., Owens, S., Gilbert, J., Schneckner, J., Wild, B.,
774 Hannisdal, B., Maerz, J., Lashchinskiy, N., Čapek, P., Šantrůčková, H., Gentsch, N., Shibistova,
775 O., Guggenberger, G., Richter, A., Torsvik, V. L., Schleper, C., and Urich, T.: Distinct microbial
776 communities associated with buried soils in the Siberian tundra, *ISME J.*, 8, 841–853, 2014.
- 777 Grosse, G., Harden, J., Turetsky, M. R., McGuire, A. D., Camill, P., Tarnocai, C., Frothing, S.,
778 Schuur, E. A. G., Jorgenson, T., Marchenko, S., Romanovsky, V., Wickland, K. P., French, N.,
779 Waldrop, M. P., Bourgeau-Chavez, L., and Striegl, R. G.: Vulnerability of high-latitude soil
780 organic carbon in North America to disturbance, *J. Geophys. Res.*, 116, G00K06,
781 <https://doi.org/10.1029/2010JG001507>, 2011.
- 782 Grosse, G., Robinson, J. E., Bryant, R., Taylor, M. D., Harper, W., DeMasi, A., Kyker-Snowman, E.,
783 Veremeeva, A., Schirmermeister, L., and Harden, J.: Distribution of late Pleistocene ice-rich
784 syngenetic permafrost of the Yedoma suite in east and central Siberia, Russia, U. S. Geological
785 Survey Open File Report, 1078, 37 pp., 2013.
- 786 Gruber, N., Friedlingstein, P., Field, C. B., Valentini, R., Heimann, M., Richey, J. E., Romero-
787 Lankao, P., Schulze, D., and Chen, C.-T. A.: The vulnerability of the carbon cycle in the 21st
788 century: An assessment of carbon-climate-human interactions, in: *The Global Carbon Cycle,*
789 *Integrating Humans, Climate and the Natural World*, edited by: Field, C. and Raupach, M.,
790 Island Press, Washington D. C., 45–76, 2004.
- 791 Hammer, Ø., Harper, D.A.T., and Ryan, P. D.: PAST: Paleontological Statistics Software Package
792 for Education and Data Analysis. *Palaentologia Electronica*, 4(1), 9 pp., 178kb, [http://palaeo-](http://palaeo-electronica.org/2001_1/past/issue1_01.htm)
793 [electronica.org/2001_1/past/issue1_01.htm](http://palaeo-electronica.org/2001_1/past/issue1_01.htm), 2001.
- 794 Harden, J. W., Koven, C. D., Ping, C. L., Hugelius, G., McGuire, A. D., Camill, P., Jorgenson, T.,
795 Kuhry, P., Michaelson, G. J., O'Donnell, J. A., Schuur, E. A. G., Tarnocai, C., Johnson, K., and
796 Grosse, G.: Field information links permafrost carbon to physical vulnerabilities of thawing,
797 *Geophys. Res. Lett.*, 39, L15704 <https://doi.org/10.1029/2012gl051958>, 2012.
- 798 Horwath Burnham, J. and Sletten, R. S.: Spatial distribution of soil organic carbon in northwest
799 Greenland and underestimates of High Arctic carbon stores, *Global Biogeochem. Cy.*, 24,
800 GB3012, <https://doi.org/10.1029/2009GB003660>, 2010.
- 801 Hugelius, G. and Kuhry, P.: Landscape partitioning and environmental gradient analyses of soil
802 organic carbon in a permafrost environment, *Global Biogeochem. Cy.*, 23, GB3006,
803 <https://doi.org/10.1029/2008GB003419>, 2009.
- 804 Hugelius, G., Kuhry, P., Tarnocai, C., and Virtanen, T.: Soil organic carbon pools in a periglacial
805 landscape: a case study from the central Canadian Arctic, *Permafrost Periglac.*, 21, 16–29,
806 <https://doi.org/10.1002/ppp.677>, 2010.
- 807 Hugelius, G., Virtanen, T., Kaverin, D., Pastukhov, A., Rivkin, F., Marchenko, S., Romanovsky, V.,
808 and Kuhry, P.: High-resolution mapping of ecosystem carbon storage and potential effects of
809 permafrost thaw in periglacial terrain, European Russian Arctic, *J. Geophys. Res.*, 116, G03024,
810 <https://doi.org/10.1029/2010JG001606>, 2011.



- 811 Hugelius, G., Strauss, J., Zubrzycki, S., Harden, J. W., Schuur, E. A. G., Ping, C.-L., Schirrmeister,
812 L., Grosse, G., Michaelson, G. J., Koven, C. D., O'Donnell, J. A., Elberling, B., Mishra, U.,
813 Camill, P., Yu, Z., Palmtag, J., and Kuhry, P.: Estimated stocks of circumpolar permafrost
814 carbon with quantified uncertainty ranges and identified data gaps, *Biogeosciences*, 11, 6573–
815 6593, <https://doi.org/10.5194/bg-11-6573-2014>, 2014.
- 816 Hugelius, G., Kuhry, P., and Tarnocai, C.: Ideas and perspectives: Holocene thermokarst sediments
817 of the Yedoma permafrost region do not increase the northern peatland carbon pool.
818 *Biogeosciences*, 13, 2003–2010, <https://doi.org/10.5194/bg-13-2003-2016>, 2016.
- 819 IPCC: Summary for Policymakers, in: *Climate Change 2013: The Physical Science Basis.*
820 *Contribution of Working Group I to the Fifth Assessment Report of the Intergovernmental Panel*
821 *on Climate Change*, edited by: Stocker, T. F., Qin, D., Plattner, G.-K., Tignor, M., Allen, S. K.,
822 Boschung, J., Nauels, A., Xia, Y., Bex, V., and Midgley, P. M., Cambridge University Press,
823 Cambridge, United Kingdom and New York, NY, USA, 2013.
- 824 Kuhry, P. and Vitt, D. H.: Fossil carbon/nitrogen ratios as a measure of peat decomposition, *Ecology*,
825 77, 271–275, <https://doi.org/10.2307/2265676>, 1996.
- 826 Kuhry, P., Dorrepaal, E., Hugelius, G., Schuur, E. A. G., and Tarnocai, C.: Potential remobilization
827 of belowground permafrost carbon under future global warming, *Permafrost Periglac.*, 21, 208–
828 214, <https://doi.org/10.1002/ppp.684>, 2010.
- 829 NCSCDv2: [Doi:10.5879/ECDS/00000002](https://doi.org/10.5879/ECDS/00000002), 2014.
- 830 Olefeldt, D., Turetsky, M. R., Crill, P. M., and McGuire, A. D.: Environmental and physical controls
831 on northern terrestrial CH₄ emissions across permafrost zones, *Glob. Change Biol.*, 19, 589–603,
832 <https://doi.org/10.1111/gcb.12071>, 2013.
- 833 Palmtag, J., Hugelius, G., Lashchinskiy, N., Tamstorf, M. P., Richter, A., Elberling, B., and Kuhry,
834 P.: Storage, landscape distribution and burial history of soil organic matter in contrasting areas
835 of continuous permafrost, *Arct. Antarct. Alp. Res.*, 47, 71–88,
836 <https://doi.org/10.1657/AAAR0014-027>, 2015.
- 837 Palmtag, J., Ramage, J., Hugelius, G., Gentsch, N., Lashchinskiy, N., Richter, A., and Kuhry, P.:
838 Controls on the storage of organic carbon in permafrost soils in northern Siberia, *Eur. J. Soil*
839 *Sci.*, 67, 478–491, <https://doi.org/10.1111/ejss.12357>, 2016.
- 840 Palmtag, J. and Kuhry, P.: Grain size controls on cryoturbation and soil organic carbon density in
841 permafrost-affected soils, *Permafrost Periglac.*, 29, 112–120, <https://doi.org/10.1002/ppp.1975>,
842 2018.
- 843 Ping, C.-L., Michaelson, G. J., Jorgenson, M. T., Kimble, J. M., Epstein, H., Romanovsky, V. E., and
844 Walker, D. A.: High stocks of soil organic carbon in North American Arctic region, *Nat.*
845 *Geosci.*, 1, 615–619, <https://doi.org/10.1038/ngeo284>, 2008.
- 846 Šantrůčková, H., Kurbatova, J., Shibistova, O., Smejkalova, M., and Kastovska, E.: Short-Term
847 Kinetics of Soil Microbial Respiration – A General Parameter Across Scales ? In: *Tree Species*
848 *Effects on Soils: Implications for Global Change*, Proceedings of the NATO Advanced Research
849 Workshop on Trees and Soil Interactions, Implications to Global Climate Change, August 2004,
850 Krasnoyarsk, Russia, pp. 229-246, https://doi.org/10.1007/1-4020-3447-4_13, 2006.
- 851 Schuur, E. A. G., Bockheim, J., Canadell, J. G., Euskirchen, E., Field, C. B., Goryachkin, S. V.,
852 Hagemann, S., Kuhry, P., Laflour, P. M., Lee, H., Mazhitova, G., Nelson, F. E., Rinke, A.,
853 Romanovsky, V. E., Shiklomanov, N., Tarnocai, C., Venevsky, S., Vogel, J. G., and Zimov, S.
854 A.: Vulnerability of Permafrost Carbon to Climate Change: Implications for the Global Carbon
855 Cycle, *Bioscience*, 58(8), 701–714, <https://doi.org/10.1641/B580807>, 2008.
- 856 Schuur, E. A. G., McGuire, A. D., Schädel, C., Grosse, G., Harden, J. W., Hayes D. J., Hugelius, G.,
857 Koven, C. D., Kuhry, P., Lawrence, D. M., Natali, S. M., Olefeldt, D., Romanovsky, V. E.,



- 858 Schaefer, K., Turetsky, M. R., Treat, C. C., and Vonk, J. E.: Climate change and the permafrost
859 carbon feedback, *Nature*, 20, 171–179, <https://doi.org/10.1038/nature14338>, 2015.
- 860 Schädel, C., Schuur, E. A. G., Bracho, R., Elberling, B., Knoblauch, C., Lee, H., Luo, Y., Shaver, G.
861 R., and Turetsky, M. R.: Circumpolar assessment of permafrost C quality and its vulnerability
862 over time using long-term incubation data, *Glob. Change Biol.*, 20, 641–652,
863 <https://doi.org/10.1111/gcb.12417>, 2014.
- 864 Shmelev, D., Veremeeva, A., Kraev, G., Kholodov, A., Spencer, R. G. M., and Walker, W. S.:
865 Estimation and Sensitivity of Carbon Storage in Permafrost of North-Eastern Yakutia,
866 *Permafrost. Periglac.*, 28, 379–390, <https://doi.org/10.1002/ppp.1933>, 2017.
- 867 Siewert, M. B., Hugelius, G., Heim, B., and Faucherre, S.: Landscape controls and vertical
868 variability of soil organic carbon storage in permafrost-affected soils of the Lena River Delta,
869 *CATENA*, 147, 725–741, <https://doi.org/10.1016/j.catena.2016.07.048>, 2016.
- 870 Siewert, M. B.: High-resolution digital mapping of soil organic carbon in permafrost terrain using
871 machine learning: a case study in a sub-Arctic peatland environment, *Biogeosciences*, 15, 1663–
872 1682, <https://doi.org/10.5194/bg-15-1663-2018>, 2018.
- 873 Schneckner, J., Wild, B., Hofhansl, F., Eloy Alves, R. J., Bárta, J., Čapek, P., Fuchslueger, L.,
874 Gentsch, N., Gittel, A., Guggenberger, G., Hofer, A., Kienzl, S., Knoltsch, A., Lashchinskiy, N.,
875 Mikutta, R., Santrůčková, H., Shibistova, O., Takriti, M., Urich, T., Weltin, G., and Richter, A.:
876 Effects of soil organic matter properties and microbial community composition on enzyme
877 activities in cryoturbated arctic soils, *PLoS ONE*, 9, e94076,
878 <https://doi.org/10.1371/journal.pone.0094076>, 2014.
- 879 Soil Survey Staff: Keys to Soil Taxonomy, Twelfth Edition, USDA Natural Resources Conservation
880 Service, Washington, D.C., 2014.
- 881 Strauss, J., Schirrmeister, L., Grosse, G., Wetterich, S., Ulrich, M., Herzsich, U., and Hubberten,
882 H.-W.: The deep permafrost carbon pool of the Yedoma region in Siberia and Alaska, *Geophys.*
883 *Res. Lett.*, 40, 6165–6170, <https://doi.org/10.1002/2013GL058088>, 2013.
- 884 Tarnocai, C., Canadell, J. G., Schuur, E. A. G., Kuhry, P., Mazhitova, G., and Zimov, S.: Soil
885 organic carbon pools in the northern circumpolar permafrost region, *Global Biogeochem. Cy.*,
886 23, GB2023, <https://doi.org/10.1029/2008GB003327>, 2009.
- 887 Vardy, S. R., Warner, B. G., Turunen, J., and Aravena, R.: Carbon accumulation in permafrost
888 peatlands in the Northwest Territories and Nunavut, Canada, *Holocene*, 10, 273–280,
889 <https://doi.org/10.1191/095968300671749538>, 2000.
- 890 Walter Anthony, K. M., Zimov, S. A., Grosse, G., Jones, M. C., Anthony, P. M., Iii, F. S. C., Finlay,
891 J. C., Mack, M. C., Davydov, S., Frenzel, P., and Frolking, S.: A shift of thermokarst lakes from
892 carbon sources to sinks during the Holocene epoch, *Nature*, 511, 452–456,
893 <https://doi.org/10.1038/nature13560>, 2014.
- 894 Weiss, N., Blok, D., Elberling, B., Hugelius, G., Jorgensen, C. J., Siewert, M. B., and Kuhry, P.:
895 Thermokarst dynamics and soil organic matter characteristics controlling initial carbon release
896 from permafrost soils in the Siberian Yedoma region, *Sediment. Geol.*, 340, 38–48,
897 <https://doi.org/10.1016/j.sedgeo.2015.12.004>, 2016.
- 898 Weiss, N., Faucherre, S., Lampiris, N., and Wojcik, R.: Elevation-based upscaling of organic carbon
899 stocks in high Arctic permafrost terrain: A storage and distribution assessment for Spitsbergen,
900 Svalbard, *Polar Research*, 36(1), <https://doi.org/10.1080/17518369.2017.1400363>, 2017.
- 901 Weiss, N. and Kaal, J.: Characterization of labile organic matter in Pleistocene permafrost (NE
902 Siberia), using Thermally assisted Hydrolysis and Methylation (THM-GC-MS), *Soil Biol.*
903 *Biochem.*, 117, 203–213, <https://doi.org/10.1016/j.soilbio.2017.10.001>, 2018.



904 Zechmeister-Boltenstern, S., Keiblinger, K. M., Mooshammer, M., Penuelas, J., Richter, A., Sardans,
905 J., and Wanek, W.: The application of ecological stoichiometry to plant–microbial–soil organic
906 matter transformations, *Ecol. Monographs*, 85, 133–155, <https://doi.org/10.1890/14-0777.1>,
907 2015.

908

909

910

911 Tables in text

912

913 Pages 21-24

914

915

916

917 Figures in text

918

919 Pages 25-30

920

921

922



923

Table 1

	Number samples	%C vs C/N	%C vs DBD	C/N vs DBD
Correlation		positive	negative	negative
PAGE21, All sites	238	0.53	0.67	0.57
CryoCarb 1-Kolyma	442	0.79	0.78	0.63
CryoCarb 2-Taymir	502	0.64	0.69	0.47
CryoCarb 3-Seida	80	0.47	0.84	0.47



924

Table 2

	Number samples	DBD vs C release/gdw	%C vs C release/gdw	C/N vs C release/gdw
Correlation		negative	positive	positive
PAGE21, All sites	238	0.52	0.45	0.34
CryoCarb 1-Kolyma	442	0.52	0.47	0.54
CryoCarb 2-Taymir	502	0.41	0.33	0.48
CryoCarb 3-Seida	80	0.81	0.43	0.38



925

Table 3

a										
	Pt	Min/CE	Min Mtn	Min Pty	Min Lowl	Alluv	Eol	Pl Yed		
PAGE21, All sites	0.20	0.29	0.99	1.51	1.44	1.43	1.68			
CryoCarb-Kolyma	4.83	6.72	17.8	15.3	19.4	22.0		11.5		
CryoCarb-Taymir	6.24			29.3	24.7	26.2				
CryoCarb-Seida	2.40			5.76	7.92					

b										
	Pt	Min/CE	Min Mtn	Min Pty	Min Lowl	Alluv	Eol	Pl Yed		
PAGE21, All sites	0.14	0.20	0.69	1.05	1	0.99	1.17			
CryoCarb-Kolyma	0.25	0.35	0.91	0.79	1	1.12		0.59		
CryoCarb-Taymir	0.26			1.18	1	1.06				
CryoCarb-Seida	0.30			0.73	1					
Mean relative lability	0.24	0.28	0.80	0.94	1	1.06	1.17	0.59		
S.D. relative lability	0.07	0.11	0.16	0.21		0.07				

Abbreviations: 'Pt' = peat deposits (Histels/Histosols); 'Min/CE' = C-enriched pockets in cryoturbated soils (Turbels); 'Min Mtn' = mineral soils in mountain settings; 'Min Pty' = peaty wetlands (mineral soils with histic horizon); 'Min Lowl' = mineral soils in lowland settings; 'Alluv' = recent alluvial deposits and Holocene soils formed in alluvial deposits; 'Eol' = recent eolian deposits and Holocene soils formed in eolian deposits; 'Pl Yed' = Pleistocene Yedomas deposits

926

Table 4

	AL_Min	AL_Ce	P_Min	P_Ce	AL_Pt	AL_OLs	AL_Min Ls	P_Min Ls	
AL_OL	< 0.001	0.0072	< 0.001	< 0.001	< 0.001	0.0493	< 0.001	< 0.001	AL_OL
AL_Min	0.5761	0.2217	0.5360	0.1887	0.1887	< 0.001	0.6598	0.5682	AL_Min
AL_Ce	0.1464	0.1387	0.5570	0.5186	0.5186	0.0160	0.1956	0.7096	AL_Ce
P_Min				0.0119	0.0119	< 0.001	0.7353	0.0809	P_Min
P_Ce				0.0119	0.0119	< 0.001	1.0000	0.1828	P_Ce
AL_Pt						0.0018	0.0518	0.1103	AL_Pt
AL_OL Ls						< 0.001	< 0.001	< 0.001	AL_OL Ls
AL_Min Ls								0.2500	AL_Min Ls

	AL_Min	AL_Ce	P_Min	P_Ce	AL_Pty	AL_Pt	P_Pt	Fr_Yed	Th_Yed	
AL_OL	0.3800	0.0027	0.0658	< 0.001	0.0255	< 0.001	< 0.001	< 0.001	< 0.001	AL_OL
AL_Min		< 0.001	0.011	< 0.001	0.0174	< 0.001	< 0.001	< 0.001	< 0.001	AL_Min
AL_Ce			0.1178	0.2318	0.8849	0.0083	< 0.001	0.3428	0.1653	AL_Ce
P_Min				< 0.001	0.1656	< 0.001	< 0.001	0.0017	< 0.001	P_Min
P_Ce				0.4539		0.0098	< 0.001	0.9258	0.2751	P_Ce
AL_Pty						0.0168	< 0.001	0.5059	0.2036	AL_Pty
AL_Pt						0.0440	< 0.001	< 0.001	0.0034	AL_Pt
P_Pt							< 0.001	< 0.001	< 0.001	P_Pt
P_Yed									0.1448	P_Yed



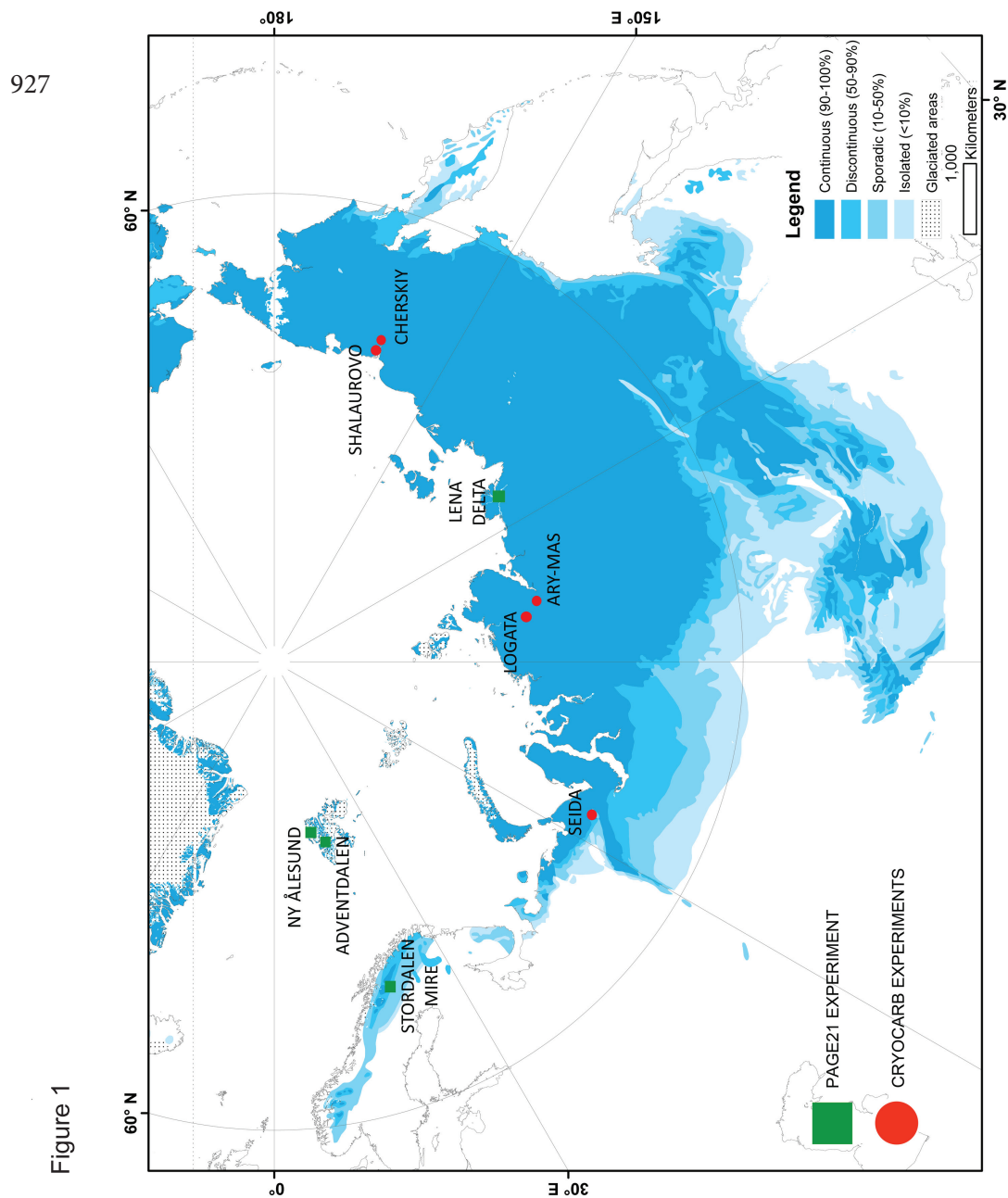
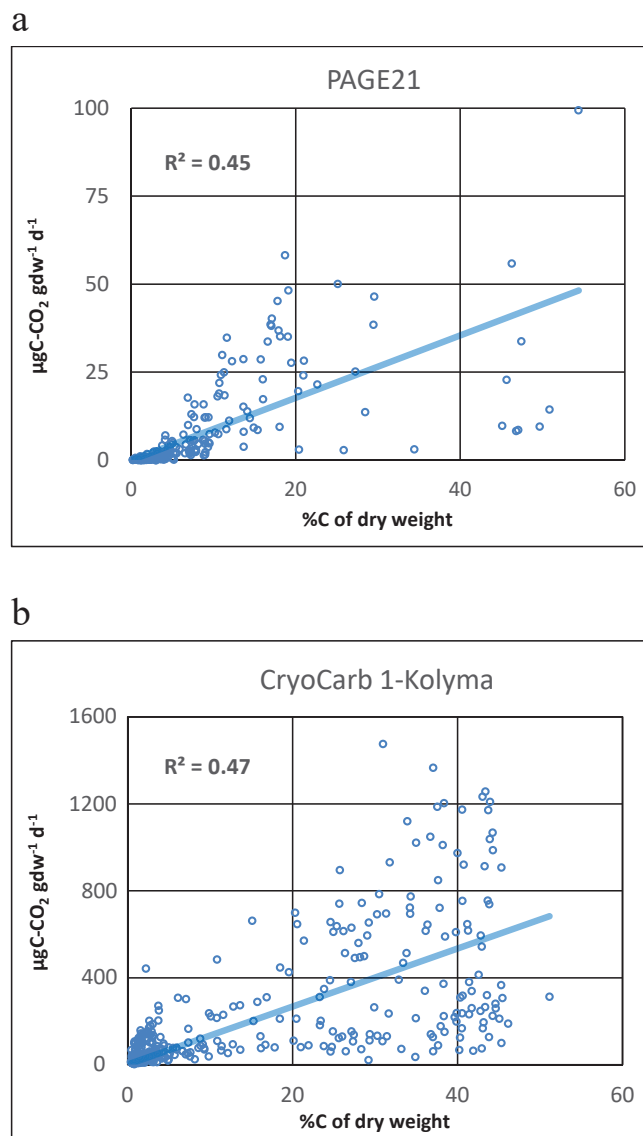




Figure 2

928

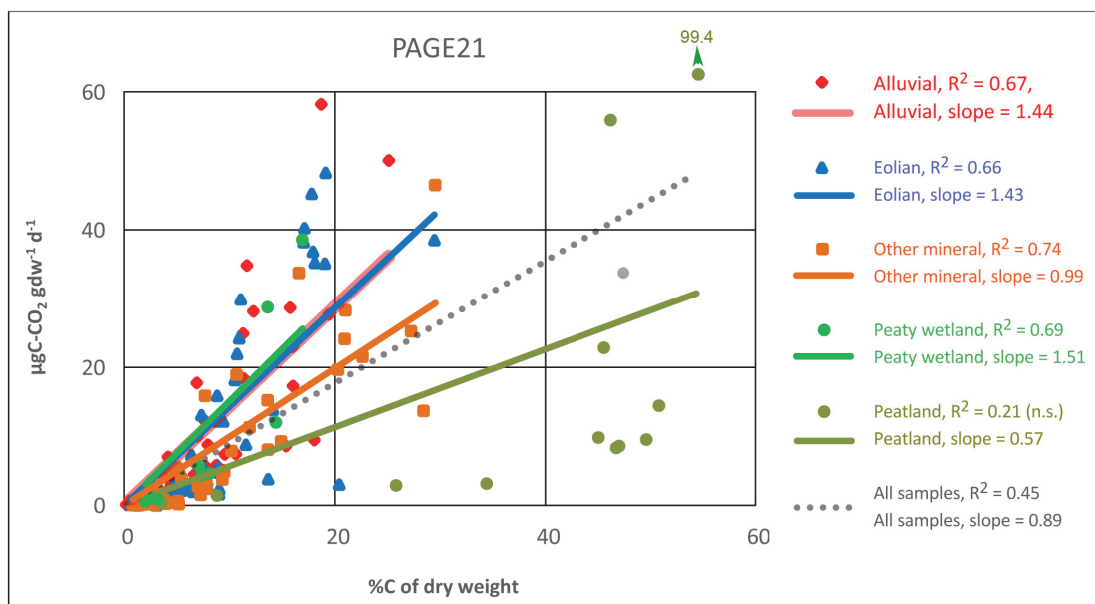




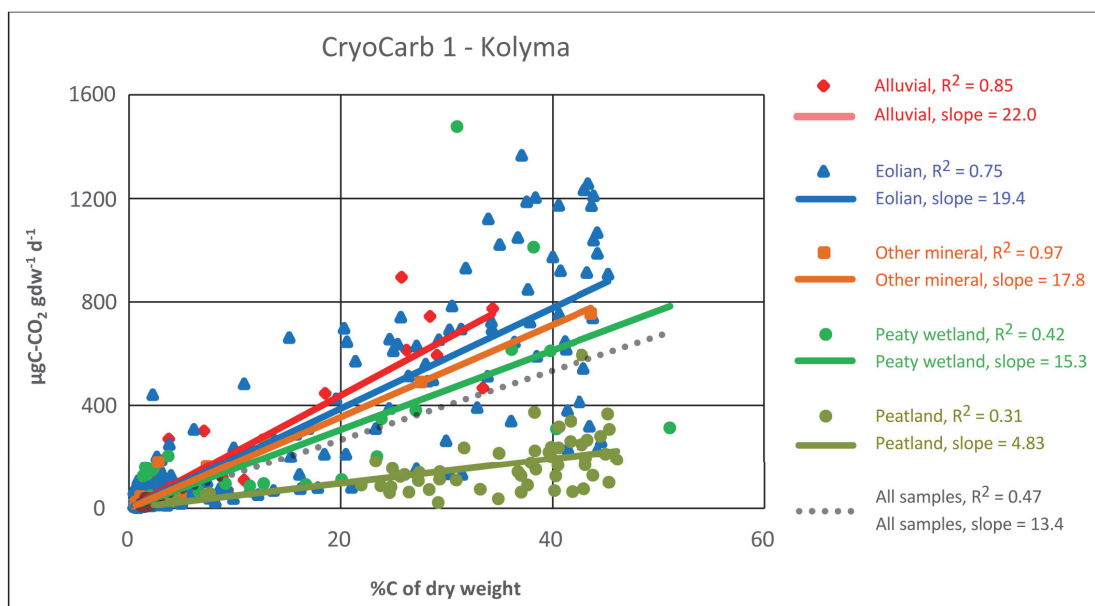
929

Figure 3

a



b





930

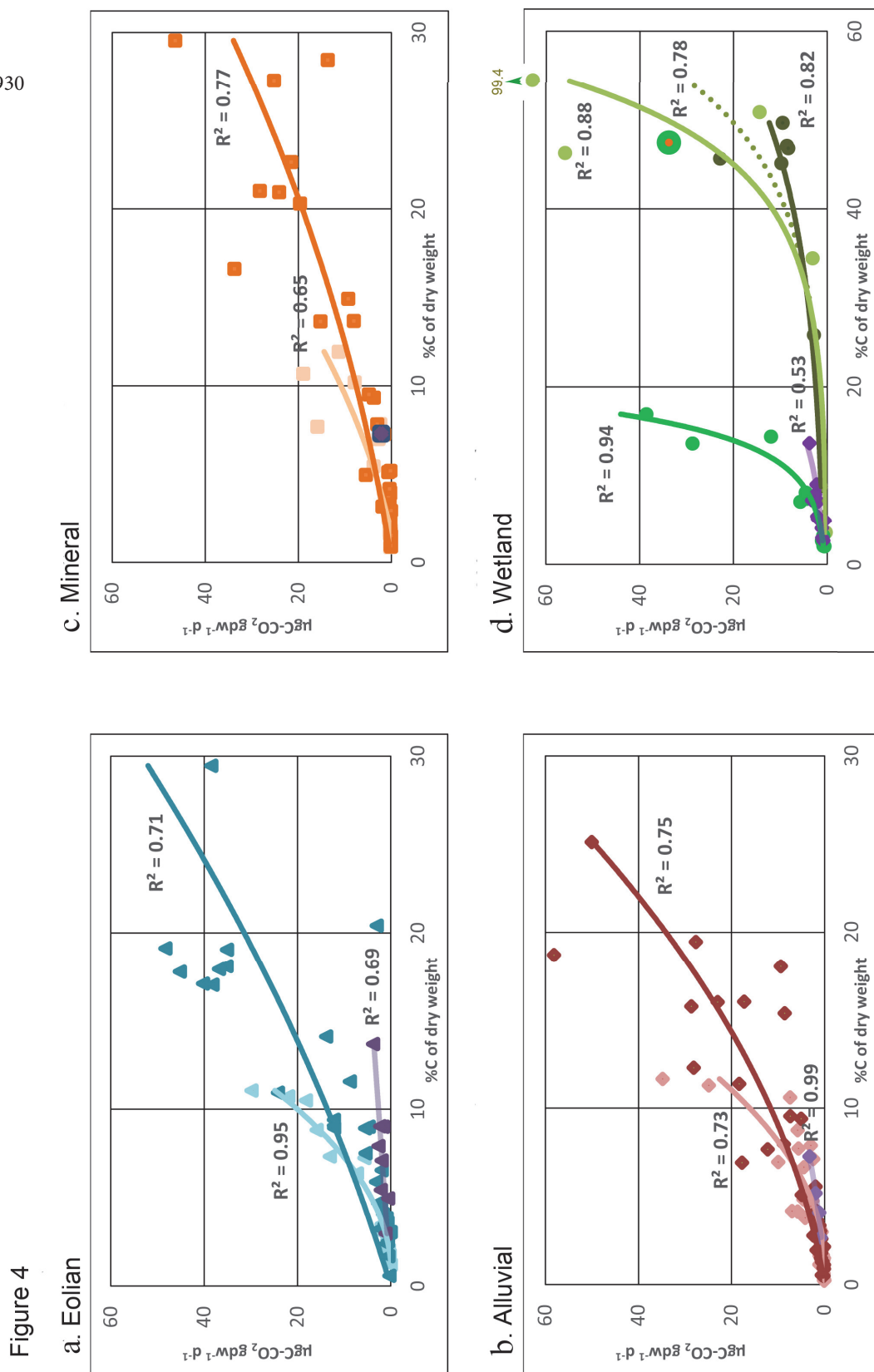
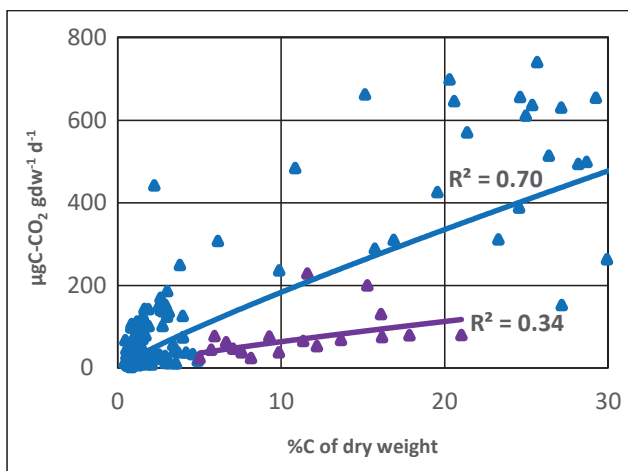




Figure 5.

a



931

b

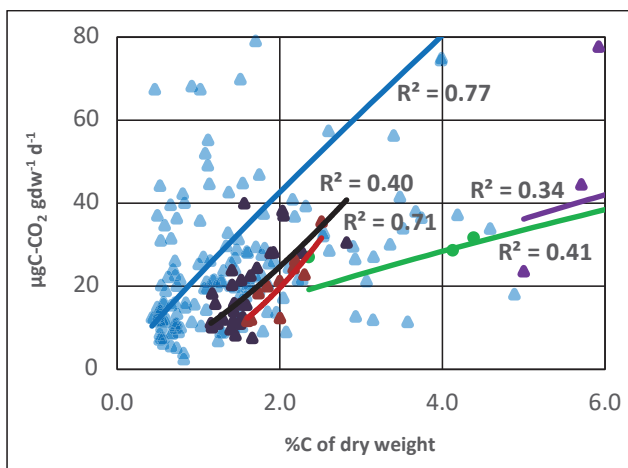




Figure 6.

